3.
TRAPEZOIDAL TOOTHED LOG-PERIODIC ANTENNA

3.1 Introduction

The details and historical developments related to trapezoidal toothed log-periodic antenna (TTLPA) are discussed in previous chapters. It is described in chapter 1 that the TTLPA has multiple elements (teeth) of trapezoidal shape which are scaled by a constant scaling factor. The TTLPA can be designed to obtain broad bandwidth where the size and number of teeth decide lower and upper frequency limits, and hence its bandwidth. A typical TTLPA with two symmetrical arms is balanced in nature and can be fed at the vertices either by a balanced two-wire line or by a coaxial cable with the outer conductor bonded to one half of the structure and inner conductor attached to another half of the structure [Duhamel and Ore (1959)]. Theoretically, two-arm balanced TTLPA has constant input impedance of approximately 188.5 Ω and generates bidirectional radiation pattern over its operating bandwidth [Duhamel and Ore (1958)]. Usually an antenna is excited using 50 Ω coaxial cable feed, which is an unbalanced type of feed. However, its performance in terms of both impedance and pattern bandwidths suffers from impedance mismatch and unbalanced nature of feed. Therefore, a balun [Kraus *et al.* (2006)] (transition between unbalanced feed line and balanced antenna) is required for proper connection of antenna to the coaxial cable feed. The balun should be designed in such a way that it provides (i) impedance matching between coaxial cable feed (having characteristic impedance of 50 Ω) and the antenna having input impedance of 188.5 Ω, and (ii) field transition over the operating bandwidth of antenna. The microstrip line (MS)-to-parallel stripline balun [Vinagamoorthy *et al.* (2012)], ultra-wideband microstrip line (MS)-to-coplanar stripline (CPS) balun [Woo *et al.* (2013)], multisection matching transformer followed by radial stub based MS-to-CPS transition [Tu and Chang (2006)] are some of the planar baluns reported in literature. Planar baluns offer flexibility in the planar circuit design and its integration with balanced antennas.

In addition, electrical size of TTLPA and hence its bandwidth can be increased through changes in antenna elements' geometry and/or conductor/dielectric loading for a given physical length/ lateral size of antenna. Viewed in another way, physical length/ lateral size of the antenna can be reduced for a given antenna bandwidth. Various techniques for bandwidth enhancement/ size miniaturization of log-periodic antennas have been reported in the literature. Different shapes of stub loading were used at the end of each element [Pirai and Hassani (2009)], [Yeo and Lee (2012)] and [Sun *et al.* (2014)] whereas in references [Elsheakh and Abdallah (2014) and Karim *et al.* (2010)], each element is modified using meander line and fractal Koch curve which increases the electrical length of each element and results in reduction of physical lateral size (dimension along the length of elements) for a given antenna bandwidth. Also, these techniques are reported for log-periodic antennas (LPAs) designed on dielectric substrate providing directional radiation patterns. Another method for size reduction of LPAs' for a given antenna bandwidth is dielectric loading. The utilization of cylindrical hat cover filled with dielectric is a good technique for physical lateral size reduction of wire LPA [Jardon-Aguilar *et al.* (2011)]. In reference [Sammeta and Filipovic (2014)], decreased turn-on frequency and hence reduction in antenna size/ enhanced bandwidth of planar LPA has been achieved using an outer ring placed on top of superstrate. Most of the techniques mentioned previously are utilized for planar antennas designed on a substrate except the technique reported in reference [Jardon-Aguilar *et al.* (2011)]. But the dielectric filled cylindrical hat cover used at the extreme location of each wire element of LPA results in size reduction in lateral direction and also slight reduction in gain. However, the changes in size of antenna affect the gain-bandwidth product which indicates that one parameter has to be compromised while improving another parameter. Therefore, an effort has been made in the present study to enhance the bandwidth of metal TTLPA through dielectric loading without significantly affecting the gain values over the frequency band of interest.

In this chapter, simulation and experimental studies on unloaded metal TTLPA excited using tapered microstrip line-to-coplanar stripline (MS-to-CPS)

transition are presented and dielectric loading as a bandwidth enhancement technique for unloaded metal TTLPA is proposed. The design and simulations are carried out using finite element method (FEM) based Ansys' high frequency structure simulator (HFSS) software. Further, the final optimized antennas along with proposed transition are fabricated and tested. The experimental results are compared with the respective simulation results.

3.2 Unloaded Metal TTLPA fed through Tapered MS-to-CPS Transition

In this section, tapered MS-to-CPS transition (balun) is proposed for excitation of TTLPA designed for frequency range 1−8 GHz and the effects of balun on the performance of designed unloaded metal TTLPA are discussed. Unloaded metal TTLPA is fed vertically through tapered MS-to-CPS transition, which consists of two sections: tapered version of multisection Chebyshev impedance transformer [Pozar (1998)] (providing impedance matching over wider bandwidth) and a quarter-wavelength long radial stub (responsible for field transition around the design frequency of radial stub) followed by CPS. Transition was designed for the antenna centre frequency of 4.5 GHz. The reflection coefficient-frequency characteristic of the proposed antenna fed through MS-to-CPS transition is compared with the characteristic of the same antenna fed through tapered microstrip-to-parallel strip balun.

3.2.1 *Design of Tapered MS-to-CPS Transition*

Figure 3.1(b) shows the geometry of tapered MS-to-CPS transition and various dimensions of the transition are listed in Table 3.1. This transition is a modified version of the transition structure proposed by Tu and Chang [Tu and Chang (2006)]. The center frequency of the transition structure is assumed to be 4.5 GHz in the design. A 50 Ω microstrip line (unbalanced transmission line) [Wheeler (1974)] is attached to coaxial cable feed on the excitation side. Width 'Wf' (= 3.0 mm) of this microstrip line is reduced to 'Wt' (= 0.14 mm) to increase its impedance from 50 Ω to 200 Ω (simulated input impedance of unloaded metal TTLPA). The theoretical input impedance of TTLPA is 188.5 Ω. The tapered line

is a tapered version of four-section quarter-wavelength Chebyshev impedance transformer (ripple level Γ_m = 0.05). The characteristic impedances of four sections from the input end are 62 Ω, 84 Ω, 118 Ω, and 160 Ω respectively. Length and impedance of each section were calculated using the formulas given in the reference [Pozar (1998)]. This tapered microstrip line is transformed to CPS using open circuited radial stub.

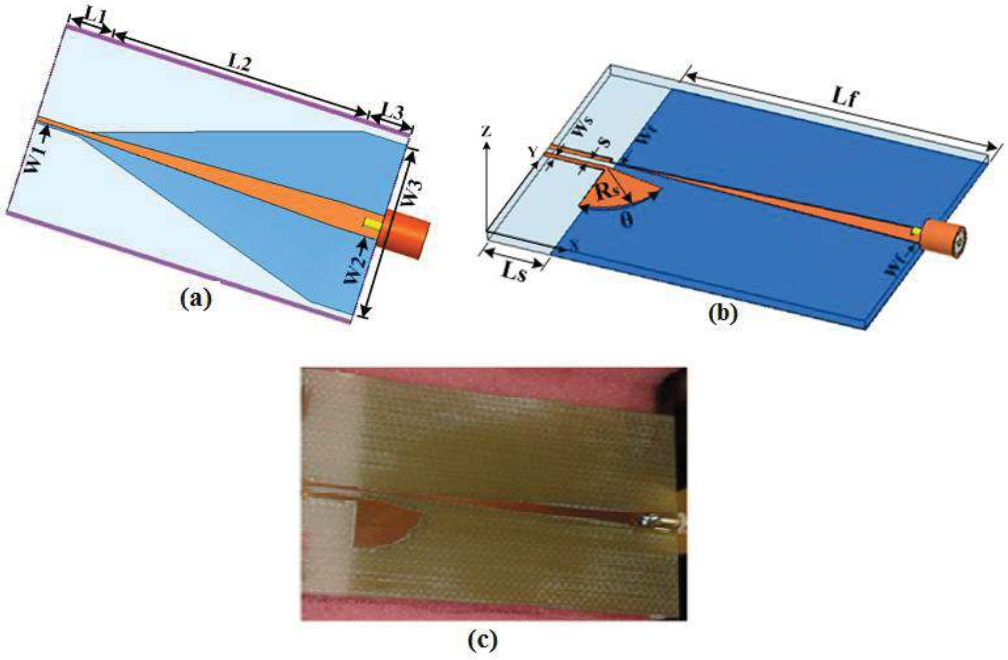

Figure 3.1: Geometry of (a) conventional MS-to-Parallel Strip balun, (b) proposed MS-to-CPS transition, and (c) prototype of MS-to-CPS transition.

Table 3.1: Design parameters of proposed MS-to-CPS transition and conventional MS-to-parallel strip line transition

Parameter	Dimension	Parameter	Dimension
Lf	47.57 mm	L1	5.0 mm
Wf	3.0 mm	L2	45.0 mm
Wt	0.14 mm	L3	5.0 mm
s	1 mm	W1	0.4 mm
Ls	9.28 mm	W2	3.0 mm
Ws	0.844 mm	W3	18.0 mm
Rs	9.28 mm	θ	80^0

The CPS is designed for characteristic impedance of 200 Ω (input impedance of antenna obtained using a lumped port between two vertices of

unloaded metal TTLPA in simulation environment) and its length 'Ls' is 9.28 mm, which is approximately equal to $\lambda_g/4$, where λ_g is the guide wavelength at 4.5 GHz. The length 'Ls' is optimized so that maximum power can be transferred to antenna terminals from the feed structure over the operating bandwidth. Length 'Lf' (= 47.57 mm) of the ground plane is same as the length of impedance transformer (sum of lengths of four sections of Chebyshev impedance transformer). Radius of radial stub 'Rs' (= 9.28 mm) is also same as the length 'Ls' (= $\lambda_g/4$) of CPS. Radial stub helps in changing the orientation of electric field. The electric field lines appearing between microstrip line and ground plane are parallel to z-axis. Electric field is rotated 90^0 due to the radial stub; hence the electric field lines between the two conductors of CPS become parallel to y-axis. Due to this field transition, currents are opposite in phase and approximately equal in magnitude (balanced mode) in CPS around the design frequency of the transition as shown in Figure 3.7. The transition was designed and fabricated using low cost FR4 substrate with a thickness 'h' of 1.6 mm and a dielectric constant ε_r = 4.4. The proposed MS-to-CPS transition with optimum dimensions was fabricated and the prototype is shown in Figure 3.1(c). To check the superiority of proposed MS-to-CPS transition, the conventional tapered microstrip-to-parallel strip balun as shown in Figure 3.1(a) was designed and used as feed for unloaded metal TTLPA. The optimum dimensions of tapered microstrip-to-parallel strip balun are listed in Table 3.1.

3.2.2 *Design of Unloaded Metal TTLPA*

The geometry of unloaded metal TTLPA along with dimensional parameters is shown in Figure 3.2(a). The antenna was designed for the frequency range 1−8 GHz. There are four teeth in the antenna structure. Longest tooth of antenna corresponding to R_1 = 75 mm is a quarter-wavelength long at the lowest design frequency f_1 = 1 GHz. The smallest tooth of the antenna corresponding to R_4 = 9.38 mm is a quarter-wavelength long at the highest frequency f_4 = 8 GHz. The lengths of remaining teeth are determined using equation (3.1), while the

widths are decided using equation (3.2) given below. The values of antenna dimensions R_1, R_2, R_3, R_4, r_1, r_2, r_3, and r_4 are given in Table 3.2.

$$\tau = \frac{f_n}{f_{n+1}} = \frac{R_{n+1}}{R_n} \tag{3.1}$$

$$\sigma = \frac{r_n}{r_{n+1}} \tag{3.2}$$

where τ (= 0.5) is geometric ratio, σ (= 0.707) is the spacing factor, $f_{n+1}>f_n$ and $R_n>R_{n+1}$. The values of parameters α, β, τ, and σ are taken from the reference [Duhamel and Ore (1958)].

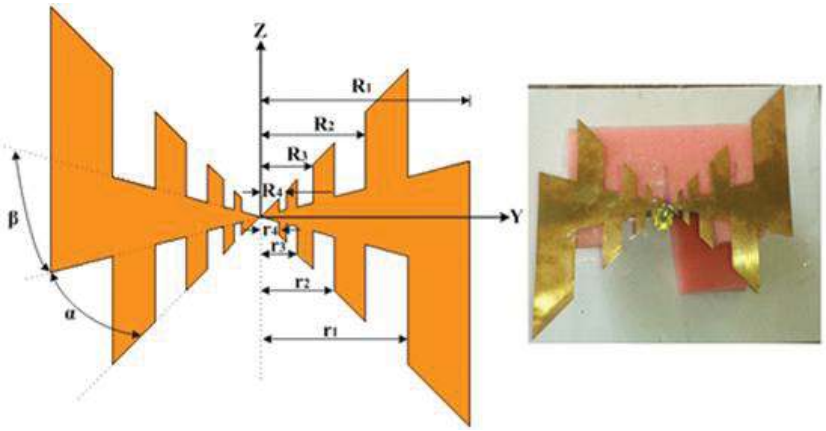

(a) (b)

Figure 3.2: Unloaded metal trapezoidal toothed log-periodic antenna (a) geometry and (b) prototype.

Table 3.2: Design parameters of unloaded metal TTLPA

Parameter	Dimension	Parameter	Dimension
R_1	75.00 mm	r_1	53.03 mm
R_2	37.50 mm	r_2	26.51 mm
R_3	18.75 mm	r_3	13.26 mm
R_4	9.38 mm	r_4	6.63 mm
α	30^0	β	30^0

The antenna is made of copper sheet having thickness of 0.2 mm and its prototype is shown in Figure 3.2(b). The antenna is oriented in yz-plane and center gap between two arms of antenna was adjusted according to the spacing between two conductors of CPS. Transition was connected vertically to the

antenna. The unloaded metal TTLPA along with different transitions and the prototype are shown in Figure 3.3.

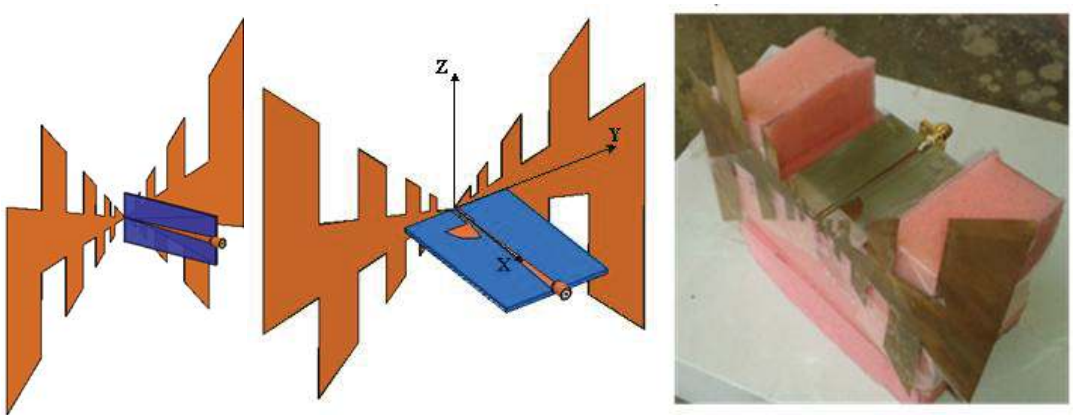

(a) (b) (c)

Figure 3.3: Configuration of unloaded metal TTLPA along with (a) MS-to-parallel strip balun, (b) MS-to-CPS transition; and (c) prototype of unloaded metal TTLPA along with MS-to-CPS transition.

3.2.3 *Simulation and Measurement of Unloaded Metal TTLPA fed through MS-to-CPS Transition*

3.2.3.1 Simulation Study

The design and simulation of unloaded metal TTLPA along with proposed MS-to-CPS transition were performed using finite element method (FEM) based Ansys' high frequency structure simulator (HFSS) software. The optimum dimensions of antenna-transition combination were found through optimization of all the design parameters which are listed in Tables 3.1 and 3.2. The antenna-transition combination with optimum dimensions was then used to obtain simulated input and far-field characteristics of the antenna including reflection coefficient-frequency characteristic, input impedance-frequency characteristic, surface current distributions, co- and cross-polar radiation patterns in principle planes, variations of realized gain and total efficiency versus frequency.

3.2.3.2 Experimental Study

After simulations, the proposed unloaded metal TTLPA and MS-to-CPS transition were fabricated. The unloaded metal TTLPA was made of copper foil of

thickness 0.2 mm which was cut using scissor in proper shape and dimensions as shown in Figure 3.2(b). The proposed MS-to-CPS transition was designed on FR-4 substrate using T-Tech make Quick Circuit QC 5000 prototyping machine. The fabrication of whole assembly was completed after proper soldering of antenna, transition and SMA connector.

After fabrication, the antenna was tested. The values of reflection coefficient over frequency range 0.7−8.4 GHz were measured using Anritsu make VNA Master Vector Network Analyzer (Model No.: MS2038C). The radiation patterns (both co- and cross-polar) of the proposed antenna-transition combination in E-plane (yz-plane) and H-plane (xz-plane) were measured in an anechoic chamber at the discrete frequencies separated by 0.5 GHz over the frequency range 2.5−6.0 GHz. SICO make pyramidal horns (designed to operate in S-, C-, and X-bands) connected to Agilent make 250 kHz−20 GHz (Model No.: E8257D) signal generator through isolator and waveguide-to-coaxial transitions for corresponding frequency bands were used as transmitting antennas for radiation pattern measurements. The proposed antenna connected to coaxial detector placed in far-field region was used as receiving antenna for measuring radiation patterns in E- and H-planes. Further, the gain values of the antenna in boresight direction were measured using comparison method (equation 3.3) in the same setup as used for radiation pattern. The standard gain horn antennas were used as reference antennas.

$$\frac{P_{RT}}{P_{RS}} = \frac{G_T}{G_S} \tag{3.3}$$

where P_{RT} and P_{RS} are the power levels received by test antenna (proposed antenna) and standard antenna (standard gain horn antenna) respectively. G_T and G_S are the gains of test antenna and standard gain horn antenna respectively.

Simulated and corresponding measured results for reflection coefficient-frequency characteristic, radiation patterns and realized gain-frequency characteristic were compared and discussed in different Sub-sections of Results and Discussion Section.

3.2.4 *Results and Discussion*

3.2.4.1 Reflection Coefficient- and Input Impedance-Frequency Characteristics

The results for the variations of simulated and measured reflection coefficients of the unloaded metal TTLPA (along with transition) with frequency are shown in Figure 3.4. It is observed from Figure 3.4 that the simulated and measured -10 dB reflection coefficient bandwidths of the structure nearly match each other.

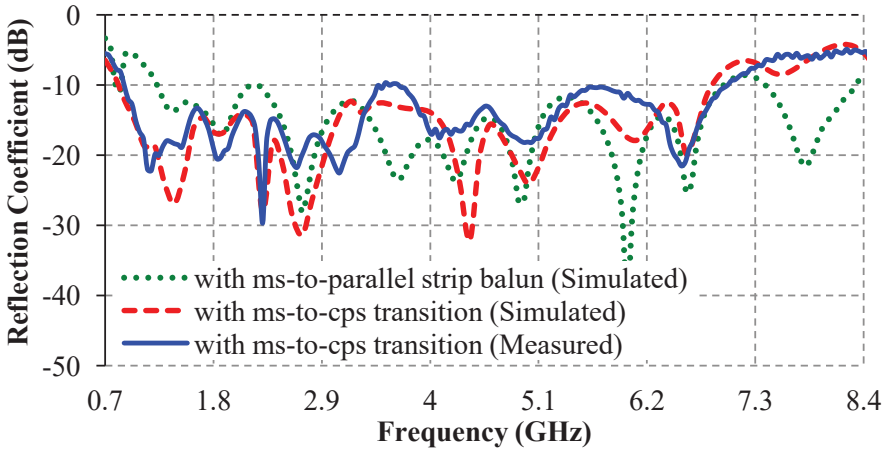

Figure 3.4: Simulated and measured reflection coefficients-frequency characteristics of the unloaded metal TTLPA (along with transition).

The simulated variation of reflection coefficient of proposed antenna along with MS-to-CPS transition versus frequency is also compared with the corresponding characteristic of same antenna fed through microstrip-to-parallel strip balun and the results are shown in Figure 3.4. The microstrip-to-parallel strip balun is tapered version of balun used in reference [Vinagamoorthy *et al.* (2012)] and was designed on 1.6 mm thick FR4 substrate having relative dielectric constant 'ε_r' of 4.4. Its dimensions, which are listed in Table 3.1 were optimized to obtain maximum impedance bandwidth. It is clear from Figure 3.5 that the -10 dB simulated reflection coefficient bandwidth of the antenna fed through microstrip-to-parallel strip balun is found to be 5.6:1 (1.25−7.0 GHz) while same antenna fed through the proposed MS-to-CPS transition provides -10 dB reflection coefficient bandwidth of 7.67:1 (0.9−6.9 GHz). This signifies that

impedance matching of the antenna fed through microstrip-to-parallel strip balun deteriorates (reflection coefficient goes above -10 dB) for frequencies lower than 1.25 GHz.

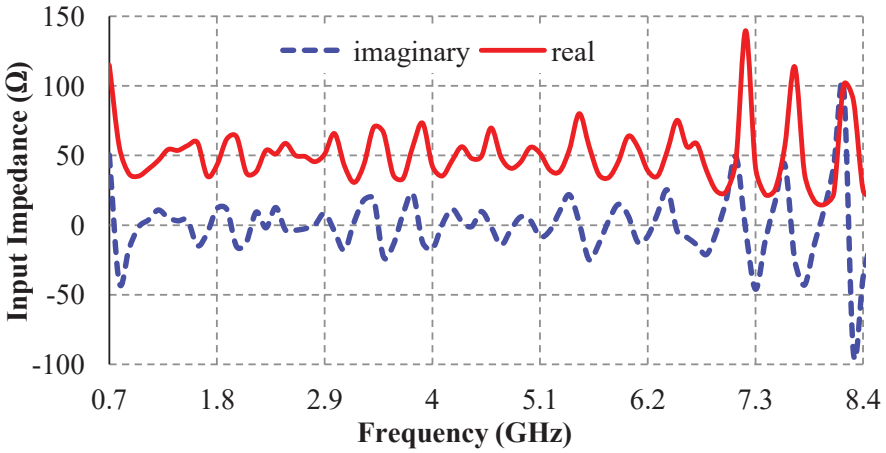

Figure 3.5: Simulated-input impedance of unloaded metal TTLPA along with transition versus frequency.

The simulated real and imaginary parts of input impedance of the antenna as functions of frequency are shown in Figure 3.5. It can be observed from Figure 3.5 that the input resistance oscillates around 50 Ω and input reactance varies around 0 Ω as frequency is varied within -10 dB reflection coefficient bandwidth of the antenna. This indicates that the input impedance of antenna is nearly matched to the 50 Ω coaxial cable feed through transition within the bandwidth of the antenna.

3.2.4.2 Simulated Surface Current Distributions

Figure 3.6 illustrates the surface current distribution on the antenna at different frequencies over the range 1−7 GHz. To understand the radiation properties of proposed antenna along with transition, surface current distributions have been shown at discrete frequencies of 1, 2, 3, 4, 4.5, 5, 6, and 7 GHz.

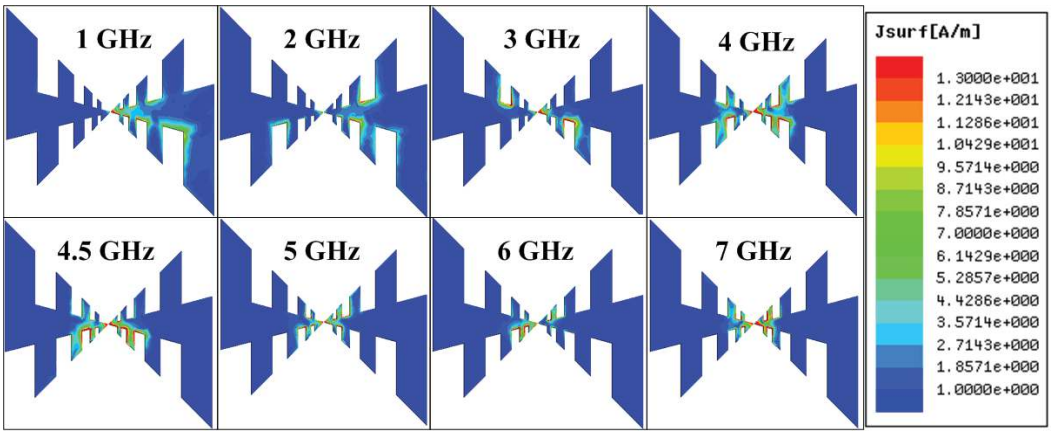

Figure 3.6: Simulated current distributions on the unloaded metal TTLPA surface at different frequencies.

It can be observed from Figure 3.6 that smaller teeth have higher surface current density as compared with other (longer) teeth at higher frequencies. Therefore, it can be said that smaller teeth resonate at relatively higher frequencies. As frequency is decreased, longer teeth start receiving higher surface current density values, which indicates that the longer teeth resonate at relatively lower frequencies within the operating frequency band. Another interesting observation is that surface current distributions on both the arms of antenna are almost identical for frequencies of 3, 4 and 4.5 GHz (the design frequency of balun). But the current distributions on the surface of two antenna arms are not identical for frequencies of 1, 2, 5, 6, and 7 GHz. It can also be verified from the current distribution on the surface of MS-to-CPS transition (Figure 3.7), which acts as exciter for the antenna. Almost identical distributions of current on both the arms of the antenna are responsible for bidirectional radiation pattern around the design frequency of balun. Hence, it can be stated that the performance of antenna is affected by balun characteristics.

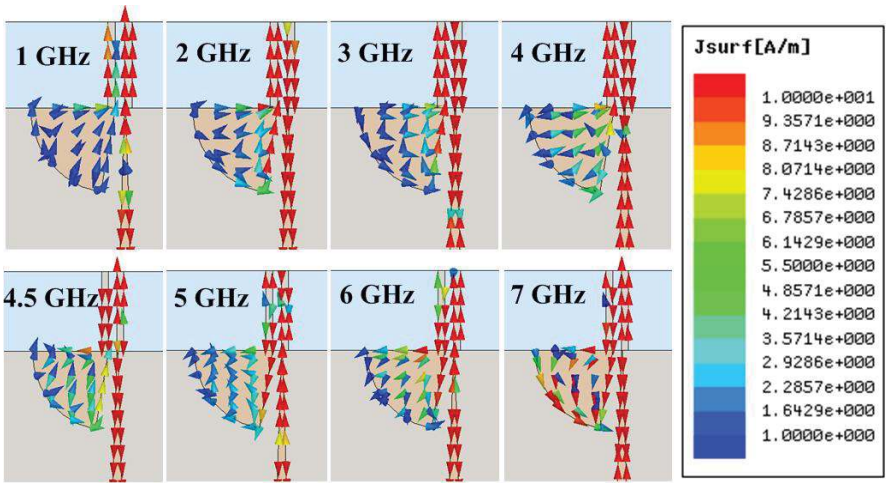

Figure 3.7: Simulated vector current distributions on MS line-to-CPS transition at different frequencies.

The vector plots of surface current distributions on MS-to-CPS transition at different frequencies are shown in Figure 3.7. It is clear from Figure 3.7 that currents in the two CPS conductors are opposite in phase and equal in magnitude (balance conditions) over the frequency range 3−4.5 GHz. At 1 GHz, currents in the two conductors are in phase and unequal in magnitude. At 2 GHz, currents are opposite in phase but unequal in magnitude. Also, at or above 5 GHz balance conditions are not satisfied. The balanced mode of fields and currents is responsible for bidirectional radiation pattern of the antenna.

3.2.4.3 Radiation Patterns

The simulated and measured E- and H-plane radiation patterns of the antenna (along with transition) at discrete frequencies separated by 0.5 GHz over the frequency range 2.5−6.0 GHz are shown in Figure 3.8. It can be observed from Figure 3.8 that simulated and measured radiation patterns of the antenna nearly match each other at different frequencies of interest. Though the TTLPA has the property of bidirectional radiation pattern but this pattern is affected by the feed system used. It can be noted from Figure 3.8 that the antenna shows similar bidirectional patterns in E-plane at 4.5 GHz. This is due to equal and opposite (in phase) current distributions in the two conductors of CPS. Note that the radial stub and CPS line lengths are each equal to $\lambda_g/4$ at 4.5 GHz (center frequency of

antenna). The radial stub is responsible for field transition from unbalanced microstrip line to balanced coplanar stripline. It is observed that radiation pattern gets distorted gradually for frequencies on either side of the center frequency (= 4.5 GHz) of the antenna. The reason for this pattern distortion is that phase and magnitude of current on the structures of two CPS conductors are not remaining equal and out of phase at these frequencies as shown in Figure 3.7.

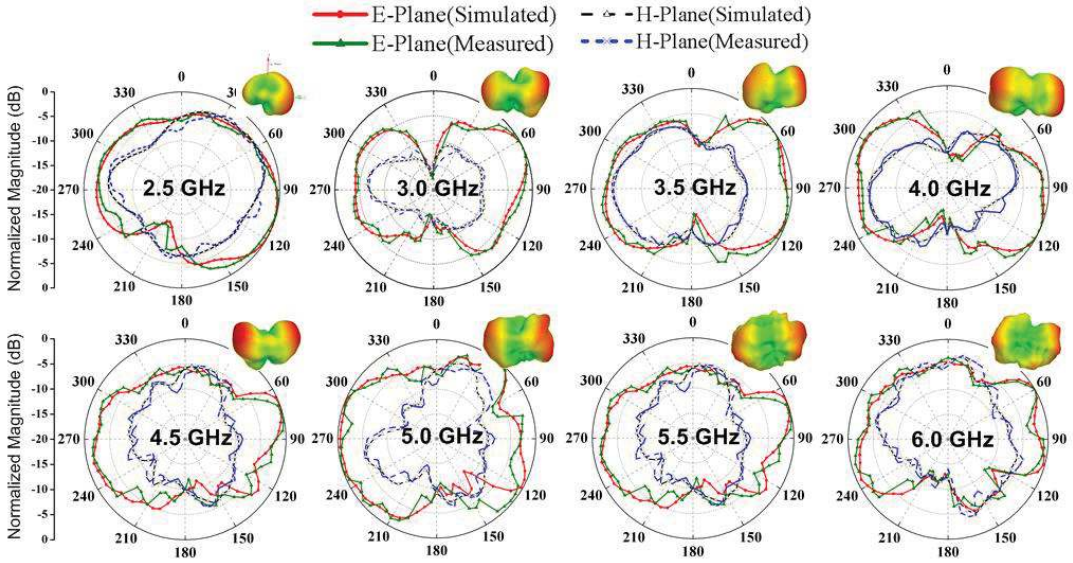

Figure 3.8: 2D (simulated and measured) and 3D (simulated) radiation patterns of the unloaded metal TTLPA (along with transition) at different frequencies.

3.2.4.4 Realized Gain- and Total Efficiency-Frequency Characteristics

Figure 3.9 shows the variations of simulated and/or measured realized gain and total efficiency of the antenna versus frequency. It can be seen from Figure 3.9 that the simulated values of antenna gain are nearly in agreement with the experimental values within the measurement frequency range. Further, simulated values of the peak realized gain of the proposed antenna (along with transition) varies from 0.25 dB (at 1 GHz) to maximum value of 5.6 dB (at 3.2 GHz) over the operating frequency band. The experimental gain values of the proposed antenna structure (along with transition) vary from 3.2 dB (at 3.5 GHz) to 5 dB (at 4.5 GHz) within the measurement frequency range 2.6−5.9 GHz. The simulated total efficiency of the antenna lies in the range 94 % (at 1 GHz) − 70 % (at 6.9 GHz).

As frequency increases, losses increase, which result in reduced total efficiency of the antenna.

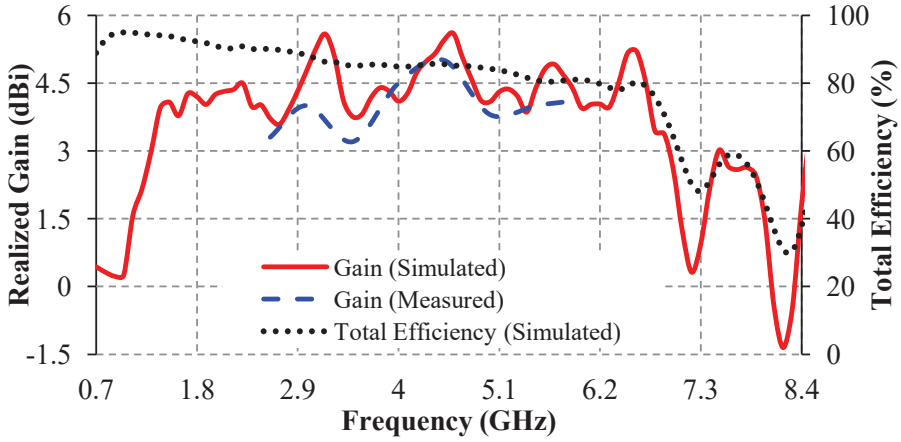

Figure 3.9: Simulated and/or measured realized gain- and total efficiency-frequency characteristics of unloaded metal TTLPA.

3.3 Dielectric-Loaded Metal TTLPA

In this section, dielectric-loaded trapezoidal toothed log-periodic antenna (DLTTLPA) is proposed and the effect of dielectric loading on performance of metal TTLPA designed for frequency range of 3−12 GHz is explained. The antenna was excited using identical MS-to-CPS transition described in previous section. The dielectric loading increases the electrical length of the antenna, thereby enhancing the bandwidth and reducing the physical size of the antenna. The input impedance of the antenna changes because of dielectric loading which leads to impedance mismatch. The balun parameters were optimized through simulation for proper impedance matching between the antenna and the feed.

3.3.1 *Design of Dielectric-Loaded Metal TTLPA*

The geometry and detailed dimensional parameters of the proposed antenna and balun are shown in Figure 3.10. The dimensions ‘R1’ and ‘R2’ of antenna with lowest and highest frequencies of 3 and 14.2 GHz were calculated using equations (3.1 and 3.2). The lengths of longest and smallest elements are one quarter-wavelength at the lowest and highest design frequencies respectively. The

metal TTLPA was designed using copper sheet having a thickness of 0.2 mm, and identical shape of Rogers RT/duroid 6010 having dielectric constant of 10.2, loss tangent of 0.0023 and thickness of 5 mm is placed on top of metal TTLPA. Owing to higher dielectric constant and thickness of material used for dielectric loading, the effective electrical length of antenna increases. Moreover, the lowest operating frequency decreases due to the increase in effective electrical length which shows size miniaturization of the antenna in terms of wavelength. Therefore, overall size of antenna reduces with increase in dielectric constant and thickness. However, the increased value of either dielectric constant or thickness also degrades the impedance matching. So, the optimum values of dielectric constant and thickness for which desired antenna bandwidth with reduced antenna size was obtained, are determined using parametric study (explained in further sub-section).

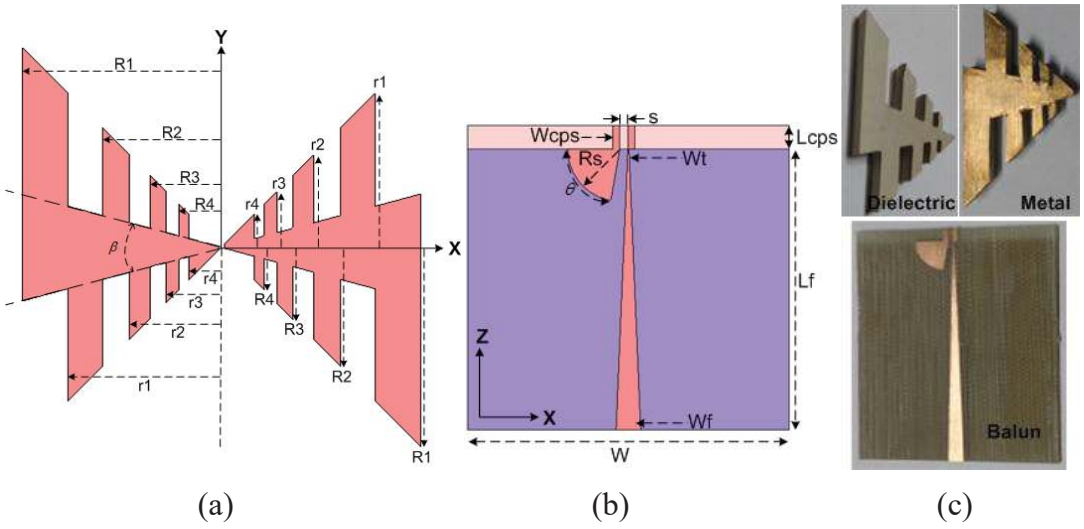

(a) (b) (c)

Figure 3.10: Geometrical configuration of (a) trapezoidal toothed log-periodic antenna, (b) MS-to-CPS transition, and (c) different parts of antenna.

The design parameters of transition are highly responsible for proper impedance matching of proposed antenna-transition combination. Therefore, the width 'Wcps' of CPS strips, and the gap 's' between strips of CPS line which also decides the separation between antenna arms are adjusted to get proper impedance matching of proposed antenna-transition combination. The design parameters with optimized dimensions of antenna-transition combination are listed in Table 3.3. Three antennas have been considered: Antenna 1 (**A1**) is an unloaded metal

TTLPA having aperture size of 48.9 × 48.9 mm^2. Antenna 2 (**A2**) is the proposed DLTTLPA having aperture size of 48.9 × 48.9 mm^2 in which the antenna is loaded with the dielectric material (Rogers RT/duroid 6010) of thickness td = 5 mm. Antenna 3 (**A3**) is again unloaded metal TTLPA having aperture size of 62.5 × 62.5 mm^2 which is larger in size than antennas **A1** and **A2** but -10 dB reflection coefficient bandwidth of antennas **A2** and **A3** are equal. The three-dimensional (3D) views of the proposed unloaded metal and dielectric-loaded metal TTLPAs are shown in Figure 3.11.

Table 3.3: Design parameters of the proposed unloaded metal and dielectric-loaded metal TTLPAs and their dimensions (unit: mm, except for β and θ)

Parameter	**A1**	**A2**	**A3**
R1	24.45	24.45	31.25
R2	14.67	14.67	18.75
R3	8.8	8.8	11.25
R4	5.28	5.28	6.75
r1	18.94	18.94	24.06
r2	11.36	11.36	14.44
r3	6.82	6.82	8.66
r4	4.1	4.1	5.19
β	30^o	30^o	30^o
W	40	40	40
Lf	35	50	35
Wf	3.06	3.06	3.06
Wt	0.14	0.14	0.14
Lcps	3	3	3
Wcps	0.844	0.844	0.844
s	1	1	1
Rs	6.5	6.5	6.5
θ	80^o	80^o	80^o
h	1.6	1.6	1.6
t	0.2	0.2	0.2
td	-	5	-

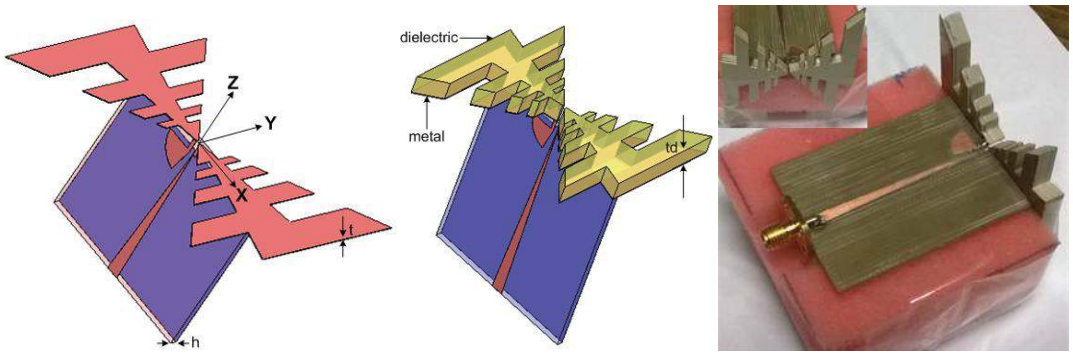

(a) (b) (c)

Figure 3.11: Three-dimensional (3D) views of proposed antenna along with transition (a) unloaded metal TTLPA, (b) dielectric-loaded metal TTLPA (antenna **A2**), and (c) prototype of antenna **A2**.

The fabrication of transition and cutting of the dielectric Rogers RT/duroid 6010 in desired shape were done using T-Tech QC5000 Quick Circuit prototyping machine. The copper sheets having proper shape and size of TTLPA were cut using scissor for fabrication of antenna **A2**. Dielectric material for antenna loading was prepared by gluing together four Rogers RT/duroid 6010 laminates each of thickness = 1.27 mm. The dielectric of thickness ~ 5 mm was then loaded on top of 0.2 mm thick copper TTLPA to transform it into the proposed DLTTLPA. Finally, the transition was connected vertically to the dielectric-loaded copper TTLPA through proper soldering. The prototype of proposed antenna is shown in Figure 3.10(c).

3.3.2 *Simulation and Measurement of Dielectric-Loaded Metal TTLPA*

3.3.2.1 Simulation Study

The procedure for simulation of DLTTLPA is similar to unloaded metal TTLPA fed through MS-to-CPS transition (see Sub-section 3.2.3) except for the frequency range of operation. The DLTTLPA along with transition was simulated using Ansys' HFSS software and optimum dimensions of the antenna were obtained. The effects of dielectric constant and thickness of loaded dielectric material on the simulated reflection coefficient-frequency characteristic of the antenna are explained through parametric study in Sub-section 3.3.2.2.

As mentioned earlier, dielectric loading can either result in size miniaturization of the antenna or reduction in its lower cut-off frequency due to increase in effective electrical length, l_{eff} of the antenna in terms of wavelength which is expressed as

$$l_{eff} = l \times \sqrt{\varepsilon_{reff}} \tag{3.4}$$

$$\varepsilon_{reff} = \frac{\varepsilon_r + 1}{2} \tag{3.5}$$

$$l_{eff} \propto \lambda_{eff} \propto \frac{1}{f_{lc}} \tag{3.6}$$

where ε_r is relative permittivity of dielectric material, l is actual length of the antenna, ε_{reff}, λ_{eff}, and f_{lc} are effective relative permittivity, effective wavelength and lower cut-off frequency pertaining to the proposed antenna respectively.

To better understand the effect of dielectric loading on the performance of antenna, parametric study was carried out. The dielectric constant 'εr' and thickness 'td' of the loaded dielectric material were taken as parameters and their effects on reflection coefficient-frequency characteristic of the antenna were observed.

3.3.2.2 Parametric Study

Figure 3.12 shows the reflection coefficient-frequency characteristic of the DLTTLPA for different dielectric constant, εr-values by keeping the thickness of dielectric material, 'td' constant at 5 mm. It is easily observed from Figure 3.12 that as the dielectric constant 'εr' of the loaded dielectric material increases from 5 to 10, the lower cutoff frequency of the antenna reduces. It is due to increase in the effective electrical length of the antenna with increase in εr-value (equations (3.3−3.5)). Further, increase in dielectric constant of dielectric material (εr) from 10 to 15 shifts the characteristic towards lower frequency side slightly with negligible change in lower cutoff frequency but impedance matching is degraded. Therefore, dielectric material of dielectric constant (εr) of 10, which corresponds to Rogers RT/duroid 6010 substrate (εr = 10.2) was taken as optimum εr-value in further study.

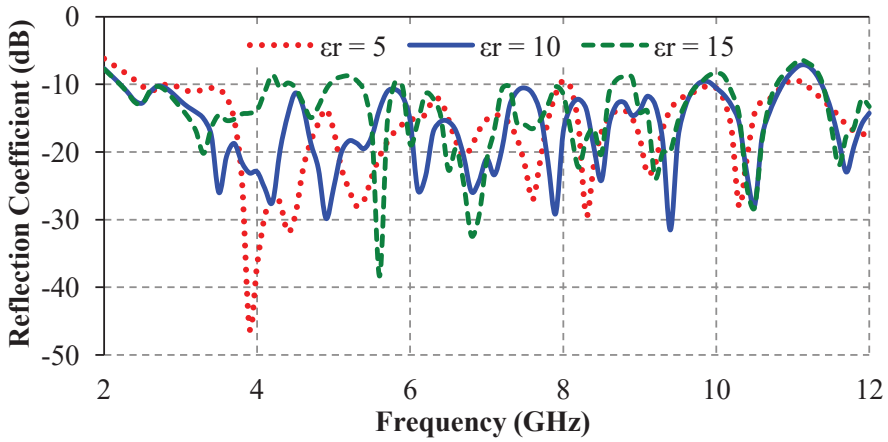

Figure 3.12: Effect of dielectric constant 'εr' of loaded dielectric material on reflection coefficient-frequency characteristic of the proposed dielectric-loaded metal TTLPA.

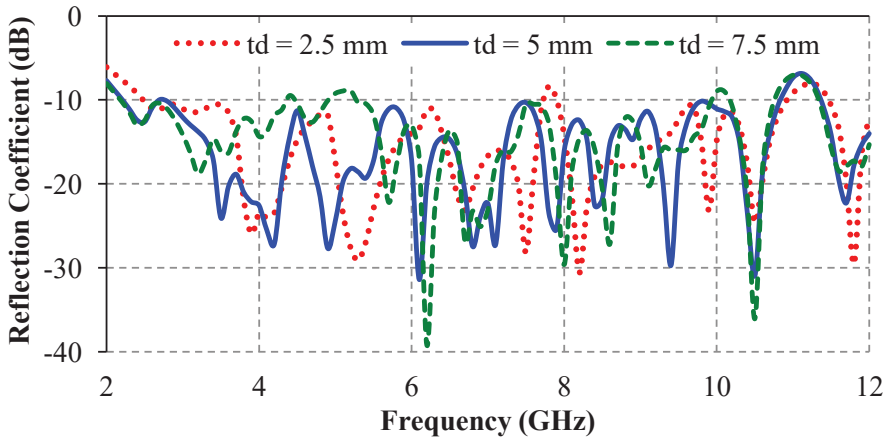

Figure 3.13: Effect of thickness 'td' of loaded dielectric material on reflection coefficient-frequency characteristic of the proposed dielectric-loaded metal TTLPA.

The effect of thickness 'td' of loaded dielectric material on the reflection coefficient-frequency characteristic of DLTTLPA is shown in Figure 3.13 in which εr-value of the loaded dielectric material is kept constant at 10.2. It can be observed from Figure 3.13 that as 'td' increases from 2.5 to 5 mm, whole operating frequency band as well as lower cutoff frequency shifts towards lower frequency side. It may due to the increase in volume of the loaded dielectric material with increase in its thickness. As 'td' is further increased from 5 to 7.5

mm, the frequency band shifts towards lower frequency side with similar lower cutoff frequency while impedance matching degrades. Along with reduced lower cutoff frequency, the impedance matching is also good over whole operating frequency range 2.2−10.8 GHz for 'td' = 5 mm as compared with 'td' values of 2.5 and 7.5 mm.

The optimum dimensions of geometrical parameters of the antennas **A1**, **A2** and **A3** were obtained through simulation as well as parametric study which are listed in Table 3.3.

3.3.2.3 Experimental Study

The proposed dielectric-loaded antenna (DLTTPA) and MS-to-CPS transition with optimum design dimensions were fabricated and measurements on fabricated antenna were performed.

The experimental procedures for DLTTLPA are similar to those for TTLPA fed through MS-to-CPS transition (see Sub-section 3.2.3.2) except for the operating frequency range. The values of reflection coefficient over frequency range of 2−12 GHz were measured using Anritsu make VNA Master Vector Network Analyzer (Model No.: MS2038C). The co-polar radiation patterns of the proposed DLTTLPA in E-plane (xz-plane) and H-plane (yz-plane) were measured in an anechoic chamber at the discrete frequencies of 5 and 7 GHz. SICO make pyramidal horns (designed to operate in S-, C-, and X-bands) connected to Agilent make 250 kHz−20 GHz (Model No.: E8257D) signal generator through isolator and waveguide-to-coaxial transitions for corresponding frequency bands were used as transmitting antennas for radiation pattern measurement. The proposed antenna connected to same VNA operating in spectrum analyzer mode and placed in far-field region was used as receiving antenna for radiation pattern measurement in E- and H-planes. Further, the experimental gain values were obtained following the procedure identical to that explained in Sub-section 3.2.3.2.

Furthermore, simulated and corresponding experimental results for reflection coefficient-frequency characteristics, radiation patterns and gain-frequency characteristic of the antenna were compared and discussed in different Sub-sections of Result and Discussion Section.

3.3.3 *Results and Discussion*

3.3.3.1 Reflection Coefficient-Frequency Characteristics of TTLPAs

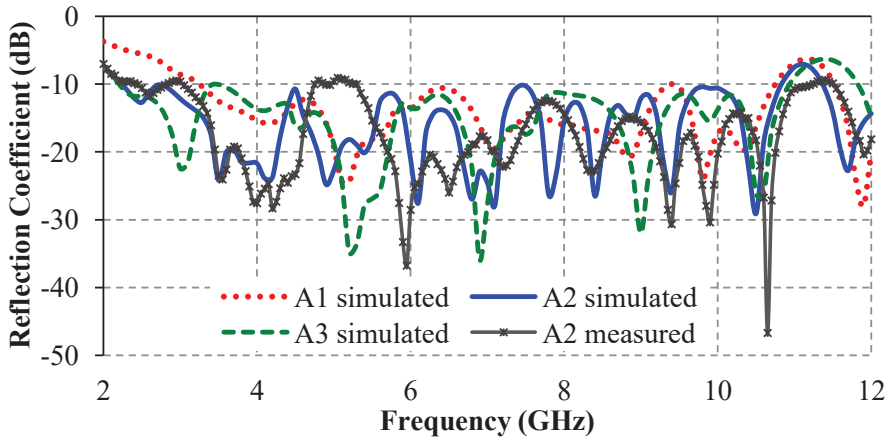

Figure 3.14: Reflection coefficient-frequency characteristics of TTLPAs.

The simulated and/or measured reflection coefficients versus frequency characteristics of proposed antennas without and with dielectric loading (antennas **A1** and **A2**) are shown in Figure 3.14. It can be seen from Figure 3.14 that **A1**, which is a metal TTLPA having aperture size of 48.9 × 48.9 mm^2 provides -10 dB reflection coefficient bandwidth of 7.6 GHz over the frequency range 3.2−10.8 GHz. **A2** is dielectric-loaded metal TTLPA having aperture size of 48.9 × 48.9 mm^2 (same as **A1**) and provides -10 dB reflection coefficient bandwidth of 8.6 GHz in the frequency range 2.2−10.8 GHz. The bandwidth comparison of **A1** and **A2** indicates that dielectric loading shifts the lower cut-off frequency towards lower frequency side without degradation in higher cut-off frequency. The antenna **A3** is a metal TTLPA with aperture size of 62.5 × 62.5 mm^2 and provides -10 dB reflection coefficient bandwidth of 8.6 GHz over the frequency range 2.2−10.8 GHz, that is identical to the bandwidth provided by antenna **A2**. Further, the comparison of aperture size of antennas **A2** and **A3** having identical

bandwidth indicates that dielectric loading reduces the antenna size without degradation in bandwidth. However, it is observed from Figure 3.14 and Table 3.3 that the proposed DLTTLPA (antenna **A2**) can either enhance bandwidth for same aperture size (when compared with antenna **A1**) or miniaturize the aperture size for same bandwidth (when compared with antenna **A3**). Also, number of resonances is increased due to dielectric loading and variations in simulated and measured reflection coefficient of the proposed DLTTLPA (antenna **A2**) with frequency are nearly in agreement as observed from Figure 3.14.

3.3.3.2 Simulated Surface Current Distributions

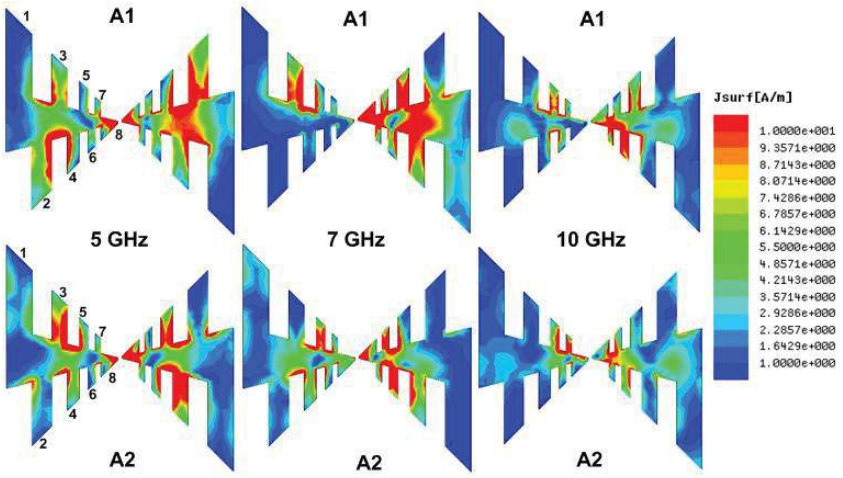

Figure 3.15: Simulated surface current distributions on antennas **A1** and **A2**.

The effect of dielectric loading can also be explained with the help of current distributions on metal surfaces of antennas **A1** and **A2**. The current distributions on surfaces of antennas **A1** and **A2** for frequencies of 5, 7 and 10 GHz are shown in Figure 3.15. It is clear from Figure 3.15 that at 5 GHz, higher levels of current are observed around all smaller elements except around the longest element of antenna **A1** and around two longer elements of antenna **A2**. At 7 GHz, six (3^{rd}–8^{th}) and five (4^{th}–8^{th}) smaller elements of antennas **A1** and **A2** respectively have higher levels of current. Similarly, five smaller elements (4^{th}–8^{th}) of antenna **A1** and four smaller elements (5^{th}–8^{th}) of antenna **A2** accommodate higher levels of surface current at 10 GHz. But the elements of antennas **A1** and **A2** have same dimensions as mentioned in Table 3.3.

Meanwhile, it is observed from Figure 3.15 and Table 3.3 that due to dielectric loading, smaller elements of antennas **A2** (DLTTLPA) are more active as compared to respective elements of antenna **A1** (unloaded metal TTLPA) at the frequencies of interest. Therefore, it can be investigated that dielectric loading increases the electrical length that provides same operating frequency range with smaller physical sizes of elements.

3.3.3.3 Radiation Patterns without and with Dielectric Loading

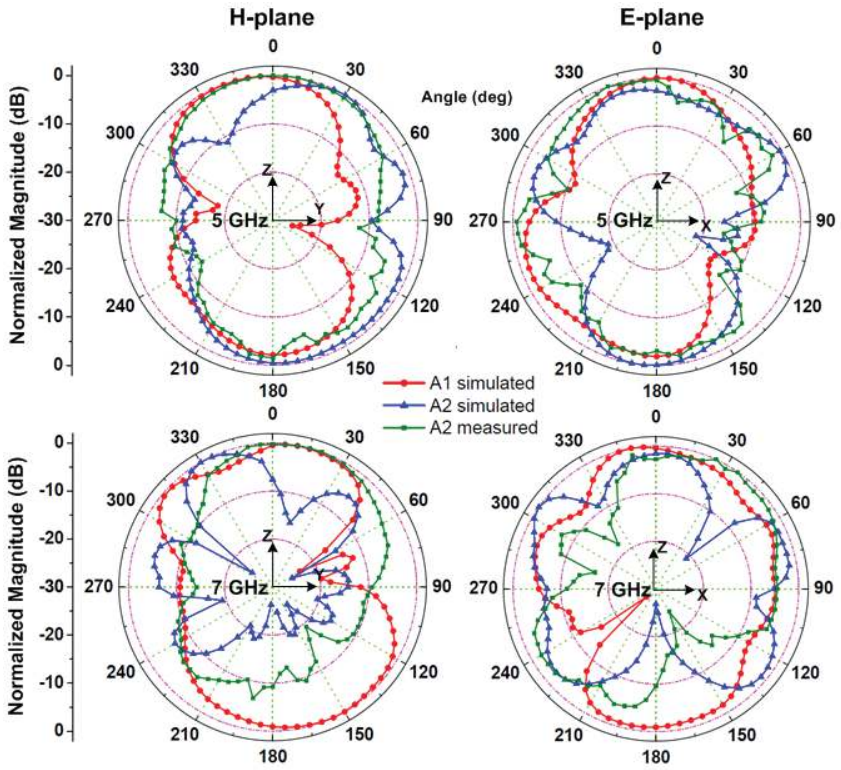

Figure 3.16: Radiation patterns of antennas **A1** and **A2**.

The effect of dielectric loading on radiation patterns of unloaded metal TTLPA was also studied through simulation as well as measurement. For such purpose, E- and H-plane radiation patterns of antennas **A1** and **A2** are compared at discrete frequencies of 5 and 7 GHz as shown in Figure 3.16. It is observed that due to dielectric loading, A2 provides more number of lobes as compared with **A1**. Further, it can be seen from Figure 3.16 that the radiation patterns in both planes are bidirectional and quite distorted from dumb-bell shape for both

antennas **A1** and **A2**. In addition, the trends of simulated and measured patterns of these antennas are nearly in agreement excepting that sharp nulls are observed in simulation results. The slight deviation in the results may due to the fabrication tolerance in terms of misalignment of both arms of fabricated antenna and the discontinuity created due to soldering material used.

3.3.3.4 Realized Gain-Frequency Characteristics without and with Dielectric Loading

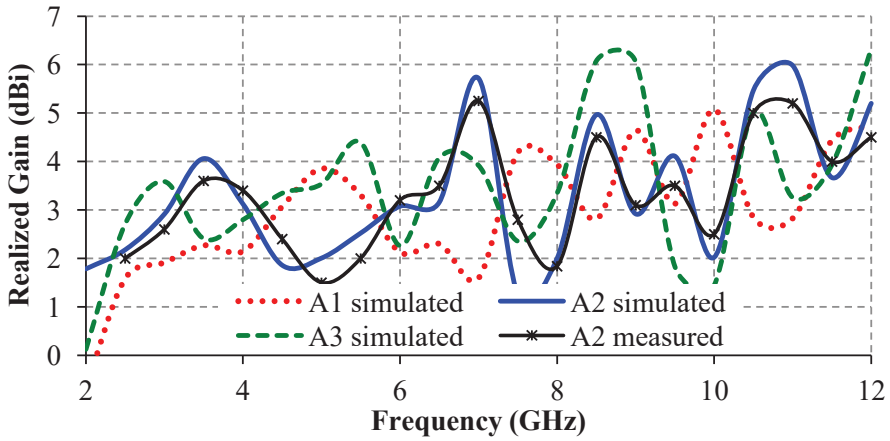

Figure 3.17: Realized gain-frequency characteristics of TTLPAs.

Figure 3.17 shows the variations of simulated and/or measured values of realized gain of antennas **A1**, **A2** and **A3** in broadside direction versus frequency. It is observed from Figure 3.17 that values of realized gain provided by antenna **A1** (which is a metal TTLPA with aperture size 48.9 × 48.9 mm^2) vary in the range 1.6−5.0 dBi over the operating frequency range 3.2−10.8 GHz. Similarly, antenna **A3** is a metal TTLPA with aperture size of 62.5 × 62.5 mm^2 and its realized gain values lie in the range 1.5−6.1 dBi over the operating frequency range 2.2−10.8 GHz. Further, it can be seen from Figure 3.17 that antenna A2 (dielectric loaded TTLPA) achieves similar values of realized gain as provided by antennas **A1** and **A3** (metal antennas without dielectric loading) and its gain values vary in the range 1.3−5.7 dBi over the operating frequency range 2.2−10.8 GHz. The variations in simulated and measured gain values of antenna **A2** with frequency are nearly in agreement. The discrepancy between simulated and

measured gain values over the frequency band of interest may be due to experimental errors.

To show that proposed dielectric loading does not degrade the gain, the characteristics of antennas **A1**, **A2**, and **A3** are compared in Table 3.4 in terms of aperture size, bandwidth and realized gain variation over their operating frequency ranges. It is investigated from Table 3.4 that proposed dielectric loading technique enhances the bandwidth and/or miniaturizes the aperture size of the proposed antenna (antenna **A2**) when compared with antennas **A1** and **A3** respectively while the range of realized gain variation is almost same.

Table 3.4: Comparison of metal TTLPAs and the proposed DLTTLPA

Parameter	**Antenna A1**	**Antenna A2**	**Antenna A3**
Aperture size	48.9 × 48.9 mm^2	48.9 × 48.9 mm^2	62.5 × 62.5 mm^2
Bandwidth	3.2-10.8 GHz	2.2-10.8 GHz	2.2-10.8 GHz
Gain	1.6-5.0 dBi	1.3-5.7 dBi	1.5-6.1 dBi

Moreover, it can be stated from this study that the proposed dielectric-loaded antenna is superior to unloaded metal TTLPA in terms of size miniaturization of overall antenna aperture by 38.78 %, bandwidth improvement by 1 GHz, (operating frequency range of proposed antenna = 2.2−10.8 GHz) for same aperture size of 48.9 × 48.9 mm^2 and similar gain variation over the operating frequency range (Table 3.4). In reference [Pirai and Hassani (2009)], only lateral dimension of the antenna studied by the investigators is reduced by 54 % through stub loading and the antenna operates over the frequency range of 2.3−8 GHz with bandwidth of 5.7 GHz and its gain varies in the range 5−6 dBi. In reference [Jardon-Aguilar *et al.* (2011)], 50 % size reduction is achieved (with tradeoff of reduced gain) for antenna loaded with cylindrical hat cover filled with dielectric which operates over frequency range of 0.9−1.4 GHz with bandwidth of 500 MHz and gain of 6.4 dBi. Therefore, it can be inferred that the proposed antenna performs better than those described in references [Pirai and Hassani (2009)] and [Jardon-Aguilar *et al.* (2011)].

3.3.3.5 *Total Efficiency-Frequency Characteristics without and with Dielectric Loading*

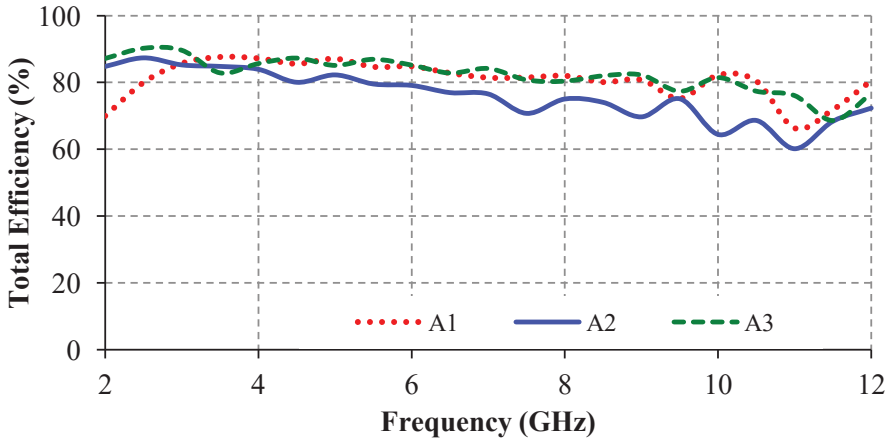

Figure 3.18: Total efficiency-frequency characteristics of TTLPAs.

The variations of simulated total efficiency-frequency characteristics of the three antennas **A1**, **A2**, and **A3** are shown in Figure 3.18. It is observed from Figure 3.18 that the total efficiency values of metal TTLPAs (**A1** and **A3**) are almost equal and more than 80 % over most of the operating frequency range. But the total efficiency values of antenna **A2** are reduced due to dielectric loading when compared with metal TTLPAs (antennas **A1** and **A3**). This reduction in total efficiency is due to higher dielectric constant of the material used for dielectric loading. The higher dielectric constant of the material increases the energy storage capacity which traps some energy within the dielectric material and decreases the radiating capacity of antenna. Still the DLTTLPA provides good total efficiency of more than 60 % (lies between 60−85 %) over the whole operating frequency range. In addition, the total efficiency of all the antennas reduces with increase in frequency. It is due to the fact that total efficiency takes into account conductor and dielectric losses within the structure of antenna. Both conductor and dielectric losses increase with frequency due to the dependence of conductor surface resistance and dielectric conductivity on frequency. Therefore, total efficiency of antenna decreases with increase in operating frequency.

3.4 Summary

In this chapter, an effort has been made to overcome the problems associated with the feed and enhance the bandwidth/ miniaturize the size of balanced metal TTLPA using balun and dielectric loading technique. The simulation and experimental studies of metal trapezoidal toothed log-periodic antenna (TTLPA) without and with dielectric loading have been presented.

At first, tapered MS-to-CPS transition has been proposed as a feed line for excitation of two-arm metal TTLPA without dielectric loading. The studies have been carried out to observe the effect of unbalanced-to-balanced (balun) feed structure along with wideband impedance transformer on the performance of balanced wideband antenna. The unloaded metal TTLPA with MS-to-CPS transition has been found to have -10 dB reflection coefficient bandwidth $\geq$ 7.67:1, which is wider as compared with the unloaded metal TTLPA excited through microstrip-to-parallel strip balun. The proposed antenna along with proposed transition generates almost bidirectional radiation patterns in the middle range of the operating frequency band, while the pattern shape gets distorted at frequencies on either side of the middle frequency range. The proposed MS-to-CPS transition is useful for the excitation of balanced wideband antenna and integration with other planar devices.

Thereafter, the dielectric loaded trapezoidal toothed log-periodic antenna (DLTTLPA) has been proposed. The effects of dielectric loading on metal TTLPA in terms of bandwidth and aperture size have been studied and investigated. It has been found through the performance comparison of the proposed and conventional antennas that dielectric loading either enhances the bandwidth or reduces the size of the antenna. These effects have been obtained because dielectric loading increases the electrical length of the antenna which shifts its lower cutoff frequency towards lower frequency side. In addition, with little increase in antenna volume antenna **A2** (DLTTLPA) has been found to provide wider bandwidth and smaller aperture size with respect to antennas **A1** and **A3** (unloaded metal TTLPAs) respectively with similar gain values, slightly

distorted radiation patterns, and reasonable total efficiency over the operating frequency range of interest.

After investigating non-planar metal TTLPA (without and with dielectric loading) in the present chapter, the bandwidth enhancement of planar monopole antenna (PMA) using curved boundary and multiple segments is taken up for investigation in the next chapter.